Research Article

Zenggui Jin, Wentao Mao and Fengpeng Yang*

Failure analysis of sandwich beams under three-point bending based on theoretical and numerical models

https://doi.org/10.1515/secm-2022-0224
received May 01, 2023; accepted September 03, 2023

Abstract: This article presents a comprehensive study on the failure behavior of foam core sandwich beams under three-point bending using theoretical analysis and finite element methods. A displacement formula for the foam sandwich beam is derived, considering the shear deformation of the foam core. Based on this formula, the deflection is obtained using energy and Rayleigh–Ritz methods. The failure loads of face yielding, core shearing, and indentation are combined to construct a failure mechanism map. The proposed theoretical model is then compared with existing theoretical analyses, demonstrating higher prediction accuracy. To investigate nonlinear damage and size effects, a series of finite element analyses is conducted. The results suggest that increasing the face sheet thickness has a greater impact on the ultimate load capacity, while the foam core thickness is more effective in enhancing bending stiffness.

Keywords: foam sandwich structure, thickness effects, failure modes, failure map, numerical simulation

1 Introduction

The foam sandwich structure, known for its lightweight, high bending stiffness, and strength, has been widely applied in marine and aerospace fields. The bending load capacity of foam sandwiches is a critical consideration for engineering applications. Therefore, understanding the bending characteristics and failure modes of foam sandwich structures is crucial for predicting their bending load capacity. Many studies have indicated that the failure behavior of foam sandwiches is closely related to the skin/core material, thickness, and interface [1–9]. Chen et al. [10] studied the plastic collapse modes of sandwich beams with aluminum foam using experimental and theoretical methods, revealing that the failure of foam sandwich beams is attributed to three primary modes: face yield, indentation, and core shear. These modes are influenced by the selection of structural geometry and material properties. McCormack et al. [3] and Ashby [11] developed the Gibson model, which can predict the critical failure loads based on various failure modes, such as face yielding, face wrinkling, core yielding, and indentation. Yu et al. [12] presented a modified Gibson model for predicting the failure modes and load history of foam sandwiches under three-point bending. This model was validated using both quasi-static and low-speed impact bending tests, confirming the accuracy of the theoretical model. Banghai et al. [13] introduced a new model for predicting the primary failure loads of foam sandwich beams under three-point bending. The model created a failure mode map that categorizes potential failure mechanisms into face yielding, core shearing, and indentation. While Jiang's model showed higher accuracy than the modified Gibson model, it was limited in analyzing and predicting thick sandwich beams due to its neglect of the shear deformation of core, which is a key factor observed in many experiments. As a result of the low shear stiffness and large thickness of the foam core, shear deformation cannot be ignored, rendering Jiang's model insufficiently accurate for describing the strain and deformation of thick sandwich beams. To address this issue, researchers have proposed various theories that consider shear deformation, including the first-order shear theory [14,15], the high-order shear theory [16,17], the layer-wise displacement theory [18,19], and the zigzag theory [20–22].

Meanwhile, researchers have made significant contributions to the field with the exploration of higher-order formulations for honeycomb-cored doubly curved shell

* **Corresponding author: Fengpeng Yang,** School of Naval Architecture, Ocean and Civil Engineering, State Key Laboratory of Ocean Engineering, Shanghai Jiao Tong University, Shanghai 200240, China, e-mail: yangfp@sjtu.edu.cn
Zenggui Jin, Wentao Mao: School of Naval Architecture, Ocean and Civil Engineering, State Key Laboratory of Ocean Engineering, Shanghai Jiao Tong University, Shanghai 200240, China

structures [23], static analysis of anisotropic doubly curved shells with arbitrary geometry and variable thickness [24], and free vibration analysis of laminated doubly curved shells with arbitrary material orientation distribution [25]. Still, the majority of these theories rest on two-dimensional models, prompting a vast body of research centered on the structural modeling of sandwich structures using two-dimensional theories [23,26–31]. Tornabene et al. have made significant contributions to this field, delving into the 3D capability of refined generalized differential quadrature models for the bending analysis of composite and sandwich plates, spherical, and doubly curved shells [26]. They also explored higher-order theories for the static and dynamic analysis of doubly curved shell structures composed of smart materials [27,31].

Nevertheless, a gap persists in understanding the influence of size effects and the inclusion of shear deformation in the core layer when predicting failure modes under three-point bending. To fill this void, this study proposes a novel semi-analytical solution, accounting for these crucial factors.

In this study, a novel semi-analytical solution for failure analysis of foam sandwich structures under the three-point bending is proposed. This theoretical model considers the shear deformation of the core layer and uses energy and Rayleigh–Ritz methods to obtain deflection. A failure map is then established by combining the failure loads of face yielding, core shearing, and indentation. Additionally, finite element analysis is conducted to investigate the nonlinear damage and size effects of the foam sandwich. The theoretical and numerical models proposed in this study can provide meaningful and valuable insights for the design and optimization of foam sandwich structures in engineering applications.

2 Theoretical analysis

Considering the case of a simply supported sandwich beam – a construction that comprises two identical face sheets and a foam core. The overall structure presents with a total length of L_0, a span length of L, uniform width denoted as b, panel thickness represented by t, and core thickness indicated by c. This particular sandwich beam construction comprises two symmetrical panels and a core layer subjected to three-point bending forces.

In terms of material properties, the face sheets possess Young's modulus and yield strength represented as E_f and σ_f, respectively. The foam core exhibits Young's modulus of E_c, a shear modulus of G_c, a compressive strength of σ_c, and a shear strength denoted by τ_c. These parameters encapsulate the key mechanical properties influencing the response of beam under load.

2.1 Analytical solution for deflection

A diagram illustrating the local deformation of a standard symmetric sandwich beam under the three-point bending is presented in Figure 1. This visualization aids in understanding the deformation behavior of beam when subjected to specific loading conditions.

Referring to Figure 1, it is possible to articulate the displacement in the longitudinal direction at any specific point within the cross-section of the beam, as represented by the equation referenced in study [32]:

$$u = u(x) = \begin{cases} \frac{c}{2}\theta - \left(z + \frac{c}{2}\right)\frac{\mathrm{d}w}{\mathrm{d}x}, & -\left(\frac{c}{2} + t\right) \le z \le -\frac{c}{2} \\ -z\theta, & -\frac{c}{2} \le z \le \frac{c}{2} \\ -\left[\frac{c}{2}\theta + \left(z - \frac{c}{2}\right)\frac{\mathrm{d}w}{\mathrm{d}x}\right], & \frac{c}{2} \le z \le \frac{c}{2} + t, \end{cases} \tag{1}$$

where w is the deflection in transverse direction, and θ is the section rotation of the core layer. This expression gives a quantitative understanding of the distribution and degree of deformation across the beam, providing crucial insights into its structural integrity and performance under load. Such understanding is critical for designing robust structures, predicting failure modes, and enhancing overall performance of materials in varying conditions. The strain in longitudinal direction can be written as:

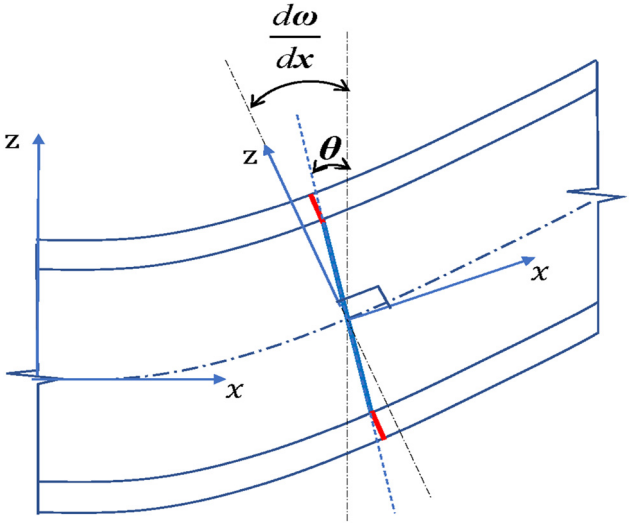

Figure 1: Schematic of sandwich beam under three-point bending.

$$\varepsilon_{xx} = \frac{\mathrm{d}u}{\mathrm{d}x} = \begin{cases} \frac{c}{2}\frac{\mathrm{d}\theta}{\mathrm{d}x} - \left(z + \frac{c}{2}\right)\frac{\mathrm{d}^2 w}{\mathrm{d}x^2}, & -\left(\frac{c}{2} + t\right) \le z \le -\frac{c}{2} \\ -z\frac{\mathrm{d}\theta}{\mathrm{d}x}, & -\frac{c}{2} \le z \le \frac{c}{2} \\ -\left[\frac{c}{2}\frac{\mathrm{d}\theta}{\mathrm{d}x} + \left(z - \frac{c}{2}\right)\frac{\mathrm{d}^2 w}{\mathrm{d}x^2}\right], & \frac{c}{2} \le z \le \frac{c}{2} + t. \end{cases} \tag{2}$$

The shear strain in transverse direction can be expressed as:

$$\gamma_{xz} = \frac{\mathrm{d}u}{\mathrm{d}z} + \frac{\mathrm{d}w}{\mathrm{d}x} = \begin{cases} \frac{\mathrm{d}w}{\mathrm{d}x} - \theta, & z \le \left|\frac{c}{2}\right| \\ 0, & \left|\frac{c}{2}\right| \le z \le \left|\frac{c}{2} + t\right|. \end{cases} \tag{3}$$

The longitudinal stress σ_{xx} and shear stress τ_{xz} are expressed as:

$$\sigma_{xx} = \begin{cases} E_f\left(\frac{c}{2}\frac{\mathrm{d}\theta}{\mathrm{d}x} - \left(z + \frac{c}{2}\right)\frac{\mathrm{d}^2 w}{\mathrm{d}x^2}\right), & -\left(\frac{c}{2} + t\right) \le z \le -\frac{c}{2} \\ -zE_c\frac{\mathrm{d}\theta}{\mathrm{d}x}, & -\frac{c}{2} \le z \le \frac{c}{2} \\ -E_f\left[\frac{c}{2}\frac{\mathrm{d}\theta}{\mathrm{d}x} + \left(z - \frac{c}{2}\right)\frac{\mathrm{d}^2 w}{\mathrm{d}x^2}\right], & \frac{c}{2} \le z \le \frac{c}{2} + t, \end{cases} \tag{4}$$

$$\tau_{xz} = \begin{cases} G_c\left(\frac{\mathrm{d}w}{\mathrm{d}x} - \theta\right), & z \le \left|\frac{c}{2}\right| \\ 0, & \left|\frac{c}{2}\right| \le z \le \left|\frac{c}{2} + t\right|. \end{cases}$$

The strain energy of whole sandwich structure, U, can be obtained as:

$$U = \frac{b}{2}\iint(\sigma_{xx}\varepsilon_{xx} + \tau_{xz}\gamma_{xz})\mathrm{d}x\mathrm{d}z. \tag{5}$$

The work done by the external force under the three-point bending is expressed as:

$$W = F \cdot w|_{\frac{L}{2}}. \tag{6}$$

The total potential energy is expressed as:

$$\Pi = U - W. \tag{7}$$

Substituting equations (2)–(6) into equation (7), the total potential energy, Π, can be expressed as:

$$\Pi = \frac{1}{2}\int_0^L \left[A_1 \cdot \left(\frac{\mathrm{d}\theta}{\mathrm{d}x}\right)^2 + A_2 \cdot \left(\frac{\mathrm{d}\theta}{\mathrm{d}x}\right)\left(\frac{\mathrm{d}^2 w}{\mathrm{d}x^2}\right) + A_3 \cdot \left(\frac{\mathrm{d}w}{\mathrm{d}x} - \theta\right)^2 + A_4 \cdot \left(\frac{\mathrm{d}^2 w}{\mathrm{d}x^2}\right)^2 \mathrm{d}x\right] - F \cdot w|_{\frac{L}{2}}, \tag{8}$$

where $A_1 = \frac{E_c bc^3}{12} + \frac{E_f c^2 bt}{2}$, $A_2 = E_f bct^2$, $A_3 = G_c bc$, and $A_4 = \frac{2E_f bt^3}{3}$.

For a three-point bending simply supported beam, the boundary conditions can be assumed as:

$$\begin{cases} w|_{x=0} = 0, & \theta|_{x=0} = \theta_0, \\ w|_{x=L} = 0, & \theta|_{x=L} = -\theta_0. \end{cases} \tag{9}$$

Considering the Rayleigh–Ritz method [19,33], the trial functions of deflection and rotation angle can be given as:

$$\begin{cases} w = w_1 \sin\left(\frac{\pi x}{L}\right) + w_2 \sin\left(\frac{3\pi x}{L}\right), \\ \theta = \theta_1 \cos\left(\frac{\pi x}{L}\right) + \theta_2 \cos\left(\frac{3\pi x}{L}\right). \end{cases} \tag{10}$$

Substituting equation (10) into equation (8) and combining the principle of minimum potential energy, the expressions are obtained as follows [33]:

$$\begin{cases} \frac{\partial}{\partial w_1}\Pi = \frac{-2L^3 A_3 \pi\theta_1 + 2L^2 A_3 \pi^2 w_1 + LA_2\pi^3\theta_1 + 2A_4\pi^4 w_1}{4L^3} - F = 0, \\ \frac{\partial}{\partial w_2}\Pi = \frac{-6L^3 A_3 \pi\theta_2 + 18L^2 A_3 \pi^2 w_2 + 27LA_2\pi^3\theta_2 + 162A_4\pi^4 w_2}{4L^3} + F = 0, \\ \frac{\partial}{\partial \theta_1}\Pi = \frac{2L^4 A_3\theta_1 - 2L^3 A_3 \pi w_1 + 2L^2 A_1\pi^2\theta_1 + LA_2\pi^3 w_1}{4L^3} = 0, \\ \frac{\partial}{\partial \theta_2}\Pi = \frac{2L^4 A_3\theta_2 - 6L^3 A_3 \pi w_2 + 18L^2 A_1\pi^2\theta_2 + 27LA_2\pi^3 w_2}{4L^3} = 0. \end{cases} \tag{11}$$

Then,

$$\begin{cases} w_1 = \frac{2FL^3(L^2A_3 + \pi^2 A_1)}{\pi^4(D_1L^2 + \pi^2 D_2)}, \\ w_2 = -\frac{2FL^3(L^2A_3 + 9\pi^2 A_1)}{81\pi^4(D_1L^2 + 9\pi^2 D_2)}, \\ \theta_1 = \frac{2FL^2\left(L^2A_3 - \frac{\pi^2 A_2}{2}\right)}{\pi^3(D_1L^2 + \pi^2 D_2)}, \\ \theta_2 = -\frac{2FL^2\left(L^2A_3 - \frac{9\pi^2 A_2}{2}\right)}{27\pi^3(D_1L^2 + 9\pi^2 D_2)}, \end{cases} \tag{12}$$

where $D_1 = A_3(A_1 + A_2 + A_4)$, and $D_2 = A_1A_4 - \frac{A_2^2}{4}$.

According to equations (10) and (12), the deflection and rotation of sandwich beam can be written as:

$$\begin{cases} w = \frac{2FL^3(L^2A_3 + \pi^2 A_1)\sin\left(\frac{\pi x}{L}\right)}{\pi^4(D_1L^2 + \pi^2 D_2)} - \frac{2FL^3(L^2A_3 + 9\pi^2 A_1)\sin\left(\frac{3\pi x}{L}\right)}{81(D_1L^2 + 9\pi^2 D_2)\pi^4}, \\ \theta = \frac{2FL^2\left(L^2A_3 - \frac{\pi^2 A_2}{2}\right)\cos\left(\frac{\pi x}{L}\right)}{\pi^3(D_1L^2 + \pi^2 D_2)} - \frac{2F\left(L^2A_3 - \frac{9\pi^2 A_2}{2}\right)L^2\cos\left(\frac{3\pi x}{L}\right)}{27(D_1L^2 + 9\pi^2 D_2)\pi^3}. \end{cases} \tag{13}$$

2.2 Failure modes

The theoretical model under discussion considers three primary failure modes: face yielding, core shearing, and indentation. Specific stress and strain distributions belong to each mode, contingent on the geometry and material properties of the sandwich beam. The following subsections delve into detailed discussions of each failure mode, offering corresponding theoretical predictions.

2.2.1 Face yield

The initiation of yield deformation in the face layer is a crucial aspect to consider. This occurs when the externally imposed stress surpasses the inherent yield strength of the material used in the face layer. The dynamic is particularly emphasized under conditions where the face layer is subjected to maximum normal stress, which, in turn, instigates plastic deformation – a permanent change in shape under applied pressure. Materials in the face layer demonstrating ideal elasto-plasticity – where elastic and plastic deformation phases are distinctly separated – present an intriguing case. In such materials, the transition to yielding is not immediate; rather, it transpires only when the stress on the surface layer reaches a state of perfect plasticity. In this state, the material deforms plastically without any increase in load or stress, indicating that it has yielded completely. For the face sheet, the normal stress σ_{xx} is expressed as:

$$\sigma_{xx} = \begin{cases} E_f\left(\frac{c}{2}\frac{\mathrm{d}\theta}{\mathrm{d}x} - \left(z + \frac{c}{2}\right)\frac{\mathrm{d}^2 w}{\mathrm{d}x^2}\right), \\ \left\{-\left(\frac{c}{2} + t\right) \le z \le -\frac{c}{2}, 0 \le x \le L\right\} \\ - E_f\left[\frac{c}{2}\frac{\mathrm{d}\theta}{\mathrm{d}x} + \left(z - \frac{c}{2}\right)\frac{\mathrm{d}^2 w}{\mathrm{d}x^2}\right], \\ \left\{\frac{c}{2} \le z \le \frac{c}{2} + t, 0 \le x \le L\right\}. \end{cases} \tag{14}$$

Substituting equation (13) into equation (14) and solving the equation to obtain the maximum of stress $\sigma_{xx\_\max}$, then let $\sigma_{xx\_\max} = \sigma_f$, the critical load for the face yield F_{fy} can be expressed as:

$$F_{fy} = -\frac{9\sigma_f \pi^2 (D_1 L^2 + \pi^2 D_2)(D_1 L^2 + 9\pi^2 D_2)}{10 L E_f \left(D_1 L^4 A_3 (c + 2t) + \frac{41}{5}\pi^2 L^2 \left(D_2 A_3 (c + 2t) - \frac{9(cA_2 - 4tA_1)D_1}{82}\right) - \frac{9D_2(cA_2 - 4tA_1)\pi^4}{2}\right)}. \tag{15}$$

2.2.2 Core shear

The foam core layer, acting as the main bearer of shear deformation, enters a stage of failure when the exerted shear stress equals or surpasses its inherent shear strength. This marks a critical transition in failure modes of the material, signifying impending structural impairment. For such a foam core layer, shear stress is defined by specific parameters. Grasping the nature of this shear stress becomes crucial, as it has a direct bearing on the structural performance under analysis. Regularly assessing the proximity of shear stress to the shear strength of material offers vital insights into the stability of the material and the likelihood of imminent failure. The distinct attributes of the foam, including density, cell morphology, and the base material, contribute significantly to its shear strength. These inherent characteristics, when interacting with the external forces to which the foam is subjected, have the potential to influence the failure point of the foam core layer. For the foam core layer, the shear stress is given as:

$$\tau_{xy} = G_c\left(\frac{\mathrm{d}w}{\mathrm{d}x} - \theta\right), \quad \left\{\frac{c}{2} \le z \le \frac{c}{2}, 0 \le x \le L\right\}. \tag{16}$$

Substituting equation (13) into equation (16) and solving the equation to determine the maximum of shear stress $\tau_{xy\_\max}$, then let $\tau_{xy\_\max} = \tau_c$, the critical load of core shear F_{cs} can be determined as:

$$F_{cs} = \frac{3\pi\tau_c (D_1 L^2 + 9\pi^2 D_2)(D_1 L^2 + \pi^2 D_2)^{\frac{3}{2}}}{2\sqrt{2} L^2 G c (2A_1 + A_2)(D_1 L^2 + 5\pi^2 D_2 2)^{\frac{3}{2}}}. \tag{17}$$

2.2.3 Indentation

Indentation represents a specific, localized mode of failure, predominantly observed in sandwich structures composed of comparatively thicker cores and slender face sheets. This form of failure typically occurs in concert with phenomena such as core yield and plastic deformation, marking a significant progression in material distress. An extensive body of theoretical analysis, represented in the

cited studies [3,7,10,34–36], has aimed to decode the intricacies of indentation failure in sandwich structures. These studies cast light on the underlying mechanisms of this failure mode, examining a myriad of factors, including the distinct properties of the materials, the architectural design of the structures, and the circumstances under which loading is applied. As a result of these meticulous investigations [3,12,13], a calculation for the critical load inducing indentation has been proposed. This critical load serves as a pivotal threshold, demarcating the point at which a material structure starts to buckle under indentation. Comprehension of this critical threshold is fundamental for predicting when sandwich structures may fail under various load conditions, thereby guiding optimizations in design processes. Based on these studies [3,12,13], the critical load of indentation is given in the following:

$$P_{\text{in}} = 2bt\sqrt{\sigma_f \sigma_c}. \tag{18}$$

2.3 Theoretical model validation

In order to verify the effectiveness of the proposed theoretical model, a symmetrical sandwich beam composed of two identical aluminum panels and aluminum foam core material is chosen as the research object. Its material properties are selected to be the same as those in the previous study [12], as shown in Table 1. The total length L_0 is 300mm, span length L is 250mm, and width b is 30mm.

A failure mode map has been constructed for a sandwich beam with an aluminum face layer and an aluminum foam core subjected to three-point bending. Using equations (15), (17), and (18), the map is constructed with t/L and c/L as its non-dimensional coordinates. The map includes three failure modes: face yielding, core shearing, and indentation. Figure 2 shows the comparison between the present model, Jiang's model [13], and the modified Gibson model [12]. In Figure 2, FY represents the face yield mode, CS represents the core shear mode, and IN represents the indentation mode.

Based on the observations made from Figure 2, it is evident that Jiang's model, the modified Gibson model, and the proposed model in this study all exhibit good agreement with the experimental results in each case. When the dimensionless parameter t/L approaches to zero, no significant changes in the transition lines between face yielding and indentation were observed in the modified Gibson model. However, both the proposed model and Jiang's model suggest that the initial failure of a sandwich structure with a thin face sheet should be due to local indentation. Although the proportion of each failure mode in the three models is slightly different, the proposed model predicts a higher proportion of core shear failure compared to Jiang's model and the modified Gibson model. The reason is that Jiang's model and the modified Gibson model are derived from the Euler–Bernoulli beam theory without considering the shear deformation of the core layer. Therefore, they overestimate the equivalent bending stiffness of the sandwich beam, leading to an overestimation of the shear failure load.

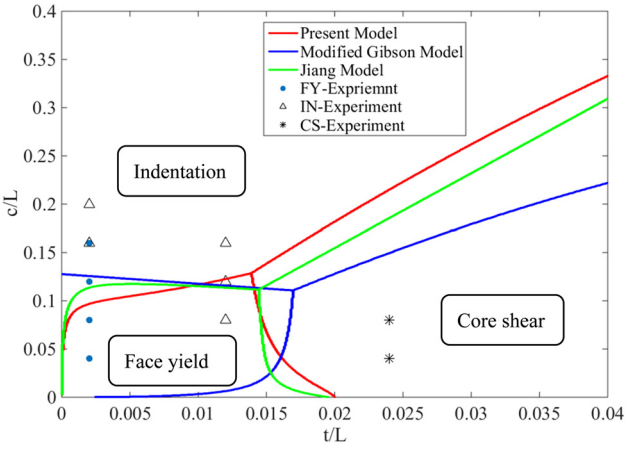

Figure 2: Comparison of experimental results and different theoretical results.

Figure 3 shows a comparison between the predicted failure loads of three theoretical models (the present model, Jiang's model, and the modified Gibson model) and experimental results obtained from three-point bending tests. In Figure 3, S0.5-C10 means a sandwich beam with 0.5 mm face sheet and 10 mm foam core, and the others are the same as this. $\bar{p}$ represents the relative load, equaling to P/P_{exp}.

From Figure 3, it can be concluded that the proposed model is more accurate in predicting the failure load compared to Jiang's model and the modified Gibson model. For thin sandwich beams, Jiang's model and the modified Gibson model underestimate the load capacity of the foam sandwich beam. In contrast, the present model's predicted values are closer to the experimental results. For sandwich beams with thick panels, the core shearing mode occurs. Jiang's model and the modified Gibson model overestimate

Table 1: Mechanical properties of face sheet and core layer [12]

Face sheets	**Material**	**LF21 aluminum alloy**
	Young's modulus	E_f **= 57 GPa**
	Yield strength	σ_f **= 92 MPa**
Foam core	Material	Closed-cell aluminum foam
	Relative density	0.17
	Young's modulus	E_c = 0.65 GPa
	Shear modulus	G_c = 0.12 GPa
	Shear strength	τ_c = 2.7 MPa

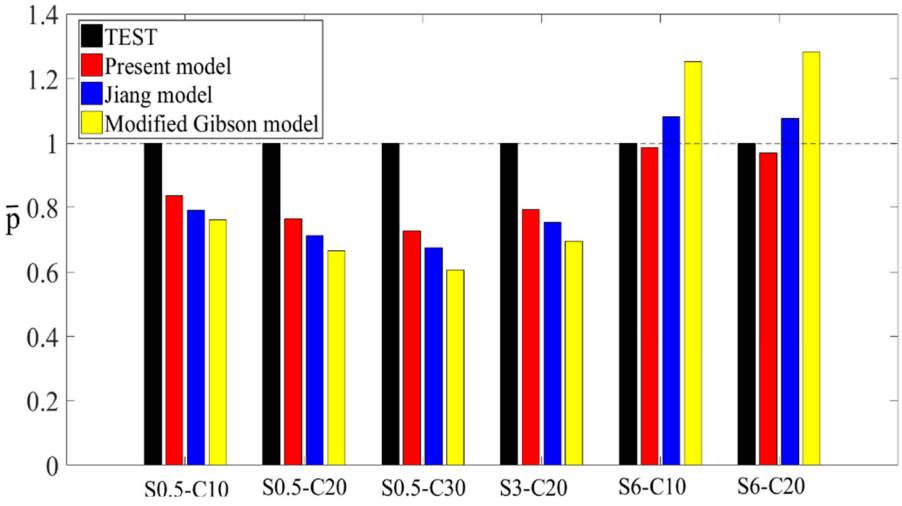

Figure 3: Comparison of experimental and theoretical results about failure loads.

the failure loads. However, the predicted results of the present model have better agreement with the experimental results.

3 Finite element analysis

The nonlinear damage problem is one of the major challenges in the failure of sandwich beams under bending, and it often involves the combination of various damage modes. Theoretical models have their limitations when it comes to predicting the nonlinear damage issues. Therefore, a numerical model based on ABAQUS was developed to simulate the nonlinear response of sandwich beams under the three-point bending. The necessary material parameters for simulation can be found in Table 1 [12]. The indenter and support are cylinders with a radius of 5 mm and are simulated by the R3D4 element. The skin part and the core part are simulated by the C3D8R element. The "TIE" constraint is used between the skin part and the core part. According to the convergence analysis of the finite element method, the mesh size of the core and panel is determined to be 2 mm × 2 mm × 4 mm, and appropriate refinement is applied in the loading area, as shown in Figure 4.

3.1 Constitutive model

The aluminum plate was simulated using an elastic–plastic constitutive model, and isotropic hardening was used. The engineering stress–strain curve and hardening curve of the aluminum plate for the tensile test are presented in Figure 5.

The foam core is simulated using a crushable foam model based on volumetric hardening. This model incorporates an elliptical yield surface composed of Mises stress and hydrostatic stress. The yield surface can be described by [37,38]:

$$F = \sqrt{q^2 + \alpha^2(p - p_0)^2} - B = 0 \tag{19}$$

Then,

$$\begin{cases} p_0 = \dfrac{p_c - p_t}{2}, \\ B = \alpha \dfrac{p_c + p_t}{2}, \\ \alpha = \dfrac{3k}{\sqrt{(3k_t + k)(3 - k)}}, \\ k = \dfrac{\sigma_c^0}{p_c^0}, \quad k_t = \dfrac{p_t}{p_c^0}. \end{cases} \tag{20}$$

where q is the Mises stress, p is the hydrostatic stress, p_c is the hydrostatic compressive yield stress, p_t is the

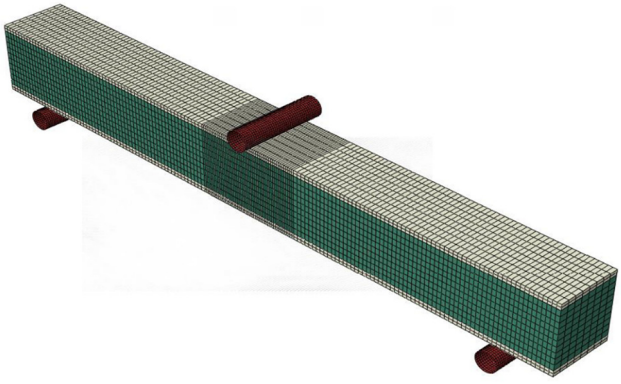

Figure 4: Schematic diagram of meshes.

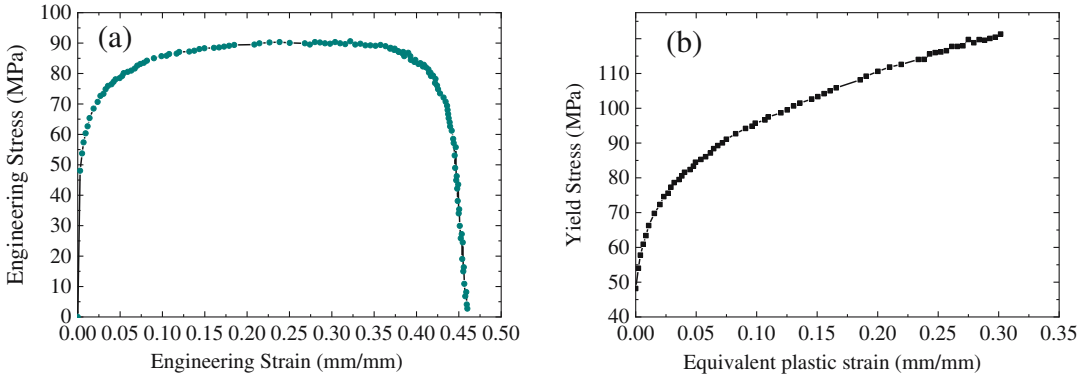

Figure 5: Aluminum panel: (a) stress–strain curve and (b) hardening curve.

hydrostatic tensile yield stress, σ_c^0 is the initial uniaxial compressive yield stress, and p_c^0 is the initial hydrostatic compressive yield stress. By defining k and k_t, the yield surface shape of the foam materials can be determined and the material hardening is described by the evolution of the yield surface shape. The evolution of the yield surface shape can be expressed by the evolution of the yield surface size on the hydrostatic pressure axis. The yield stress at hydrostatic pressure, p_c, describes the evolution of the yield surface size and is given as:

$$p_c(\varepsilon_{\text{vol}}^{pl}) = \frac{\sigma_c(\varepsilon_{\text{axial}}^{pl})\left[\sigma_c(\varepsilon_{\text{axial}}^{pl})\left(\frac{1}{\alpha^2}+\frac{1}{9}\right)+\frac{p_t}{3}\right]}{p_t+\frac{\sigma_c(\varepsilon_{\text{axial}}^{pl})}{3}}. \tag{21}$$

p_c can be obtained from the uniaxial compressive stress–strain, as shown in Figure 6.

3.2 FEA model validation

The results obtained from the finite element model calculations are compared with experimental data [12]. Figure 7 illustrates a comparison of load–displacement curves between the simulation and experimental data of three specimens: S0.5-C10, S3-C30, and S6-C10 (where S0.5-C10 denotes a skin thickness of 0.5 mm and a core thickness of 10 mm, and similarly for the other specimens). It can be observed in Figure 7 that the load–displacement curves obtained from the numerical calculations exhibit good agreement with the experimental results. During the elastic–linear stage, the finite element analysis and experimental results show good agreement, providing strong evidence of accuracy of the finite element method in predicting the bending stiffness of the sandwich beam. It is observed that there are some slight deviations between the finite element and experimental results in the nonlinear damage stage. This can be attributed to the simplification of the core material as a macroscopically uniform solid in the finite element method, which overlooks the intricacies of the foam cells. Overall, the load–displacement paths predicted by finite element analysis show good agreement with the experimental results.

Figure 8 illustrates a comparison of failure modes between finite element simulations and experimental results [12]. It is evident from Figure 8 that the failure patterns predicted by the finite element simulations and the observed experimental phenomena are highly similar under different failure modes. Specifically, indentation failure occurs when the core layer is thick,

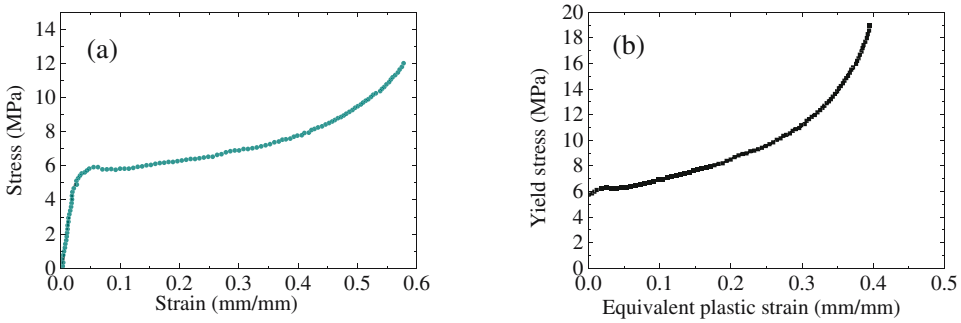

Figure 6: Foam core: (a) stress–strain curve and (b) hardening curve.

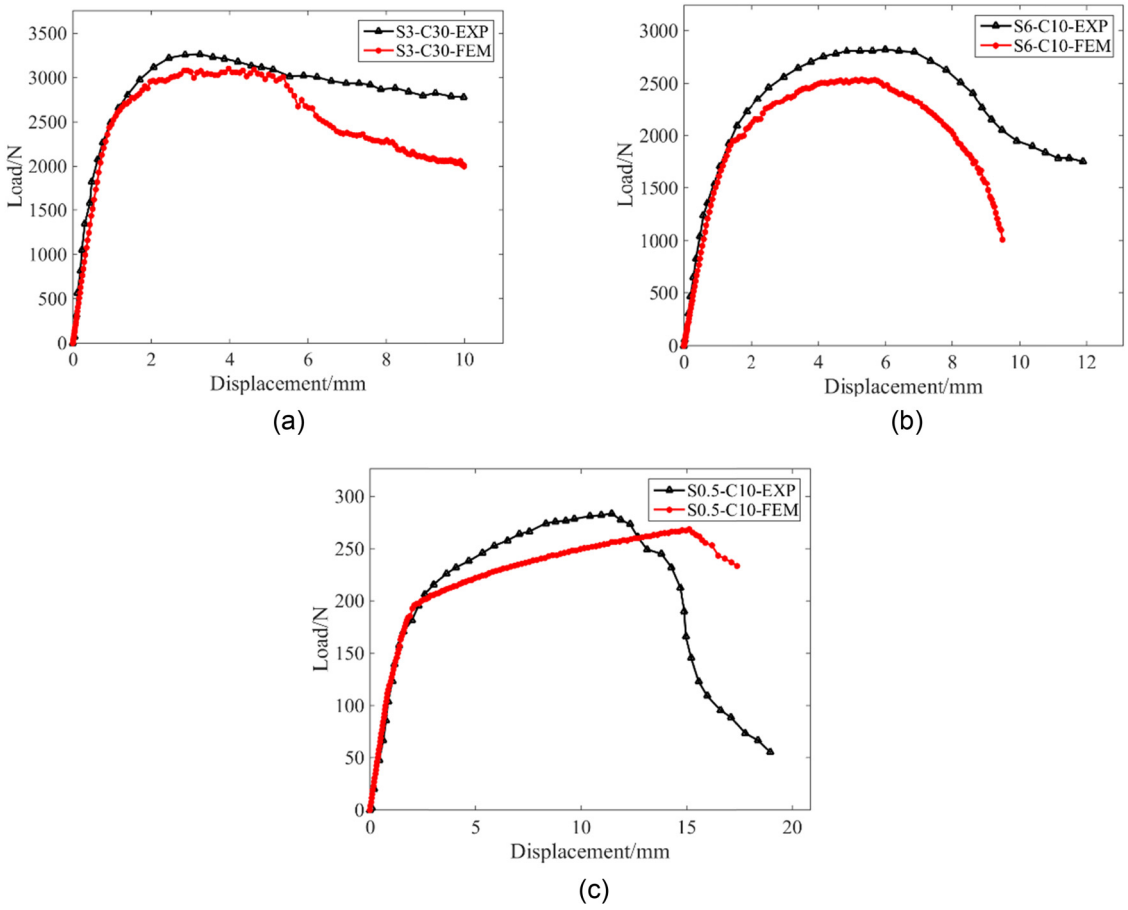

Figure 7: Comparisons of load history for experiment and simulation. (a) S3-C30, (b) S6-C10, and (c) S0.5-C10.

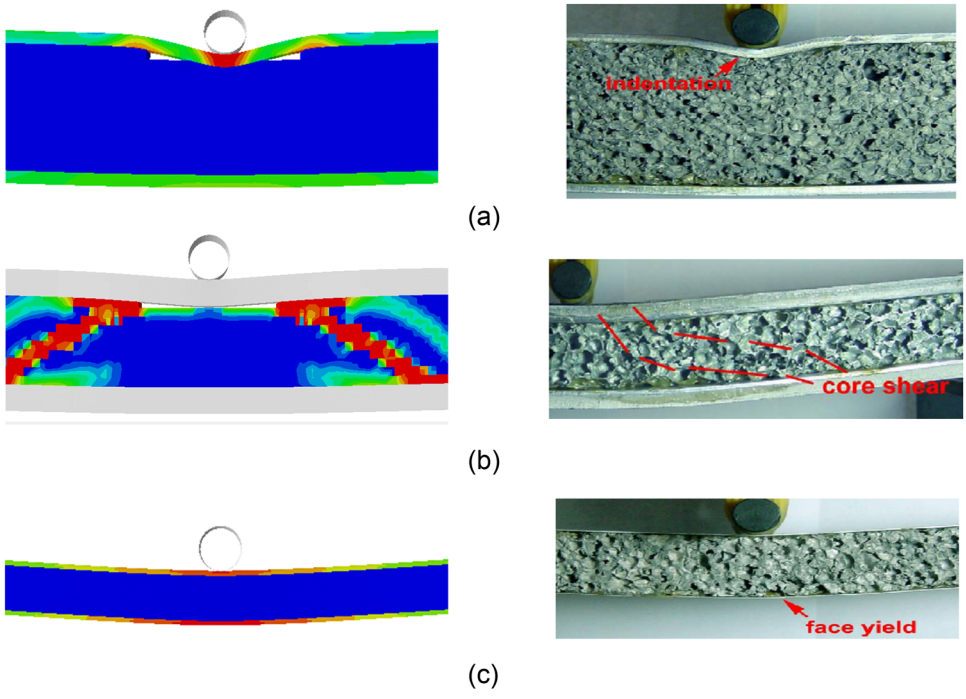

Figure 8: Comparison of finite element and experimental damage modes: (a) indentation, (b) core shear, and (c) face.

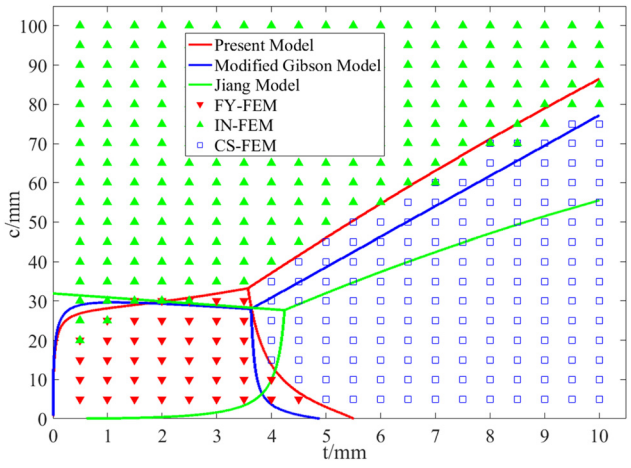

Figure 9: Comparison of finite element failure modes and theoretical models.

while core shear failure occurs when the panel is thick. Face yield failure occurs when both the panel and the core layer are thin. These results indicate that the finite element simulations are in good agreement with the experimental results for the failure modes of sandwich beams with varying thicknesses. Therefore, the proposed finite element model accurately predicts the load–displacement paths and failure modes of sandwich beams.

3.3 Effect of thickness

To investigate the effect of the thickness of face sheets and foam core on the non-linear failure behavior, a batch of modeling and analyses were conducted using the finite element software ABAQUS. The face sheet thickness is ranged from 0.5 to 10 mm with a 0.5 mm interval, and the core thickness is ranged from 5 to 100 mm with a 5 mm interval. Other parameters have been described in the previous section.

The failure modes with varying thicknesses from finite element simulations are compared with the theoretical predictions, as shown in Figure 9. The results suggest that the proposed theoretical model in this study provides better agreement with the finite element simulation results than Jiang's model and the modified Gibson model, particularly in terms of the transition lines of the three modes. The numerical results also indicate discrepancies from the

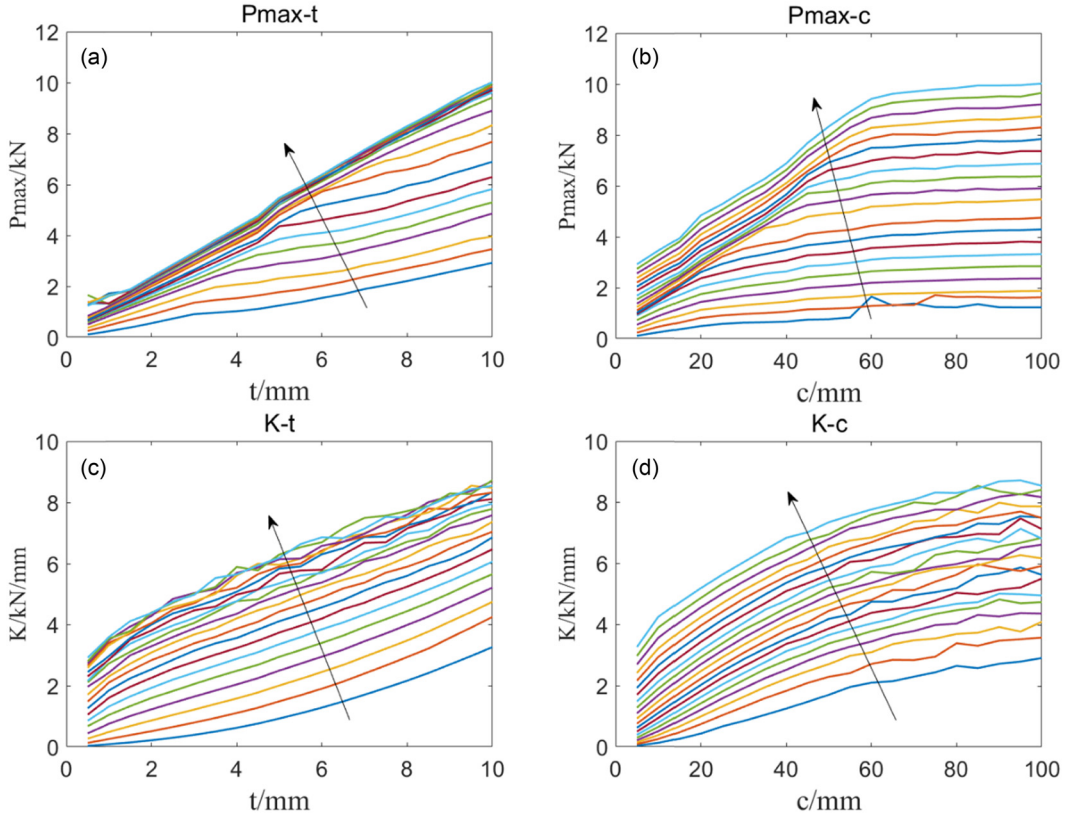

Figure 10: Bending stiffness and ultimate load vary with changes in the thickness of the core and panel: (a) ultimate load–panel thickness curves, (b) ultimate load–core thickness curves, (c) bending stiffness–panel thickness curves, and (d) bending stiffness–core thickness curves.

theoretical models, especially near the transition lines. Near the transition lines, failures of sandwich beams usually result from a combination of multiple failure modes.

Figure 10 illustrates the variation trends of bending stiffness and ultimate load with changes in the thickness of the core and face panels. The arrows in the figure indicate the direction of thickness increase. As observed in Figure 10(a), as the thickness of the sandwich beam panel grows, its ultimate load capacity also increases. This is because thicker panels can more evenly distribute loads and pressure, reducing stress and strain in specific areas. When the panel thickness is thin, there is often a concentration of loads, resulting in excessive stress in specific areas, which affects the overall load capacity. It can be seen from Figure 10(b) that for sandwich beams, as the core thickness raises, its ultimate load capacity will also increase. However, it should be noted that as the core thickness continues to enlarge, the growth trend gradually decreases. This is related to the characteristics of the sandwich structure itself, because when the core thickness is very large, the strength of the sandwich beam is already strong enough and cannot continue to grow rapidly, leading to a decreasing growth trend. From these results, the ultimate load capacity of sandwich beams is greatly affected by the thickness of the panels. When the panel thickness is increased, the bearing capacity of the sandwich beam can be effectively enhanced. This result is consistent with the results obtained from existing theoretical models [1,2,10,39]. According to Figure 10(c) and (d), as the thickness of the core layer and panel of sandwich beams raises, the bending stiffness of sandwich beams also increases. This is because the thickness of the core layer and panel greatly enhances the overall strength of the sandwich beam, enabling it to better withstand external forces and thus improve its bending stiffness. Specifically, the influence of core layer thickness on bending stiffness is greater than that on ultimate bearing capacity. The reason is that the bending stiffness of sandwich beams depends on the combination of bending stiffness of their core and panels. Among these two, the bending stiffness of the core is one of the decisive factors, and the bending stiffness increases with the thickness of the core. Therefore, increasing core thickness is an effective method to improve the bending stiffness of sandwich beams.

4 Conclusion

This study presents a theoretical model and a finite element model to predict the three-point bending failure of sandwich beams with a soft core. The theoretical model incorporates the shear deformation of the core under three-point bending and derives the deflection equation using the Rayleigh–Ritz method and energy method. It also determines the critical loads for different failure modes and constructs a failure mode diagram that includes panel yielding, core shear, and indentation to describe the competition mechanism between different failure modes. Compared to previous theoretical models, the proposed model demonstrates higher accuracy. The finite element model uses an isotropic elastic–plastic constitutive model for the panel and a crushable foam model for the core. Validation of the model is conducted by comparing the simulation results with experimental data, and it exhibits good capability in predicting the nonlinear failure behavior of sandwich beams. Additionally, the finite element model investigates the effects of thickness on bending stiffness and ultimate load of sandwich beams. The results reveal that increasing the panel thickness has a greater impact on the ultimate load, whereas increasing the foam core thickness is more effective in enhancing the bending stiffness.

In conclusion, the main innovation of this study lies in the proposed theoretical analysis that takes into account the shear deformation of the core layer. Compared with previous theories, this approach provides higher prediction accuracy in predicting the failure of sandwich structures. These research findings provide valuable guidance for preliminary design of engineering structure and assessment of failure in sandwich structures.

Conflict of interest: Authors state no conflict of interest.

Data availability statement: The data that support the findings of this study are available from the corresponding author upon reasonable request.

References

[1] Shenhar Y, Frostig Y, Altus E. Stresses and failure patterns in the bending of sandwich beams with transversely flexible cores and laminated composite skins. Compos Struct. 1996;35:143–52.
[2] Kim J, Swanson SR. Design of sandwich structures for concentrated loading. Compos Struct. 2001;52:365–73.
[3] McCormack TM, Miller R, Kesler O, Gibson LJ. Failure of sandwich beams with metallic foam cores. Int J Solids Struct. 2001;38:4901–20.
[4] Lim TS, Lee CS, Lee DG. Failure modes of foam core sandwich beams under static and impact loads. J Compos Mater. 2004;38:1639–62.
[5] Steeves CA. Optimizing sandwich beams for strength and stiffness. J Sandw Struct Mater. 2012;14:573–95.

[6] Zhang J, Qin Q, Ai W, Li H, Wang TJ. The failure behavior of geometrically asymmetric metal foam core sandwich beams under three-point bending. J Appl Mech. 2014;81:071008.
[7] Guo L, Mao R, Li S, Liu Z, Lu G, Wang Z. The load-carrying capacity of sandwich beams in different collapse mechanisms. J Sandw Struct Mater. 2021;23:2988–3016.
[8] Yuan H, Zhang J, Sun H. The failure behavior of double-layer metal foam sandwich beams under three-point bending. Thin Wall Struct. 2022;180:109801.
[9] Yang FP, Lin QY, Jiang JJ. Experimental study on fatigue failure and damage of sandwich structure with PMI foam core. Fatigue Fract Eng M. 2015;38:456–65.
[10] Chen C, Harte A-M, Fleck NA. The plastic collapse of sandwich beams with a metallic foam core. Int J Mech Sci. 2001;43:1483–1506.
[11] Ashby MF. Metal foams: A design guide. Boston: Butterworth-Heinemann; 2000.
[12] Yu J, Wang E, Li J, Zheng Z. Static and low-velocity impact behavior of sandwich beams with closed-cell aluminum-foam core in three-point bending. Int J Impact Eng. 2008;35:885–94.
[13] Banghai J, Zhibin L, Fangyun L. Failure mechanism of sandwich beams subjected to three-point bending. Compos Struct. 2015;133:739–45.
[14] Reissner E. Finite deflections of sandwich plates. J Aeronaut Sci. 1948;15:435–40.
[15] Timoshenko SP. LXVI. On the correction for shear of the differential equation for transverse vibrations of prismatic bars. Lond Edinb Phil Mag. 1921;41:744–6.
[16] Pandya BN, Kant T. Higher-order shear deformable theories for flexure of sandwich plates – Finite element evaluations. Int J Solids Struct. 1988;24:1267–86.
[17] Reddy JN. A simple higher-order theory for laminated composite plates. J Appl Mech. 1984;51:745–52.
[18] Toledano A, Murakami H. A composite plate theory for arbitrary laminate configurations. J Appl Mech. 1987;54:181–9.
[19] Hao JXWX. Bending property of sandwich beam based on layer-wise first-order theory. J Build Mater. 2014;17:1049–53.
[20] Arya H, Shimpi RP, Naik NK. A zigzag model for laminated composite beams. Compos Struct. 2002;56:21–4.
[21] Li X, Liu D. Zigzag theory for composite laminates. AIAA J. 1995;33:1163–5.
[22] Tessler A. Refined zigzag theory for homogeneous, laminated composite, and sandwich beams derived from Reissner's mixed variational principle. Meccanica. 2015;50:2621–48.
[23] Tornabene F, Viscoti M, Dimitri R, Aiello MA. Higher order formulations for doubly-curved shell structures with a honeycomb core. Thin Wall Struct. 2021;164:107789.
[24] Tornabene F, Viscoti M, Dimitri R. Static analysis of anisotropic doubly-curved shells with arbitrary geometry and variable thickness resting on a Winkler-Pasternak support and subjected to general loads. Eng Anal Bound Elem. 2022;140:618–73.
[25] Tornabene F, Viscoti M, Dimitri R. Free vibration analysis of laminated doubly-curved shells with arbitrary material orientation distribution employing higher order theories and differential quadrature method. Eng Anal Bound Elem. 2023;152:397–445.
[26] Tornabene F, Brischetto S. 3D capability of refined GDQ models for the bending analysis of composite and sandwich plates, spherical and doubly-curved shells. Thin Wall Struct. 2018;129:94–124.
[27] Tornabene F, Viscoti M, Dimitri R. Static analysis of doubly-curved shell structures of smart materials and arbitrary shape subjected to general loads employing higher order theories and generalized differential quadrature method. Comput Model Eng Sci. 2022;133:719–98.
[28] Tornabene F, Viscoti M, Dimitri R. Higher order theories for the free vibration analysis of laminated anisotropic doubly-curved shells of arbitrary geometry with general boundary conditions. Compos Struct. 2022;297:115740.
[29] Karamanli A, Vo TP, Civalek O. Finite element formulation of metal foam microbeams via modified strain gradient theory. Eng Comput. 2023;39:751–72.
[30] Nouraei M, Zamani V, Civalek Ö. Vibration of smart sandwich plate with an auxetic core and dual-FG nanocomposite layers integrated with piezoceramic actuators. Compos Struct. 2023;315:117014.
[31] Tornabene F, Viscoti M, Dimitri R, Rosati L. Dynamic analysis of anisotropic doubly-curved shells with general boundary conditions, variable thickness and arbitrary shape. Compos Struct. 2023;309:116542.
[32] Li Z, Zhou SG. The influence of shear on the bending properties of foam core sandwich beams. Fiber Reinf Plast/Compos. 2011;217:19–23.
[33] Reddy JN. Energy principles and variational methods in applied mechanics. 3rd edn. Hoboken, Chichester: Wiley; 2017. p. 730.
[34] Bart-Smith H, Hutchinson JW, Fleck NA, Evans AG. Influence of imperfections on the performance of metal foam core sandwich panels. Int J Solids Struct. 2002;39:4999–5012.
[35] Li Z, Zheng Z, Yu J, Qian C, Lu F. Deformation and failure mechanisms of sandwich beams under three-point bending at elevated temperatures. Compos Struct. 2014;111:285–90.
[36] Morada G, Vadean A, Boukhili R. Failure mechanisms of a sandwich beam with an ATH/epoxy core under static and dynamic three-point bending. Compos Struct. 2017;176:281–93.
[37] Deshpande VS, Fleck NA. Multi-axial yield behaviour of polymer foams. Acta Mater. 2001;49:1859–66.
[38] Deshpande VS, Fleck NA. Isotropic constitutive models for metallic foams. J Mech Phys Solids. 2000;48:1253–83.
[39] Staal RA, Mallinson GD, Jayaraman K, Horrigan DPW. Predicting failure loads of undamaged sandwich honeycomb panels subject to bending. J Sandw Struct Mater. 2009;11:73–104.